

The Absorption Spectrum and Absolute Absorption Cross Sections of Acetylperoxy Radicals, $\text{CH}_3\text{C}(\text{O})\text{O}_2$ in the near IR

Michael Rolletter¹, Emmanuel Assaf^{2,a}, Mohamed Assali², Hendrik Fuchs^{1,*},
Christa Fittschen^{2,*}

¹ Institute of Energy and Climate Research, IEK-8: Troposphere,
Forschungszentrum Jülich GmbH, D-52428 Jülich, Germany

² Université Lille, CNRS, UMR 8522 - PC2A - Physicochimie des Processus de
Combustion et de l'Atmosphère, F-59000 Lille, France

^a now at Earth System Research Laboratory, Chemical Sciences Division, National
Oceanic and Atmospheric Administration, Boulder, Colorado 80305, United States

*Corresponding authors: Christa Fittschen (christa.fittschen@univ-lille.fr)

Hendrik Fuchs (h.fuchs@fz-juelich.de)

Revised version

submitted to

Journal of Quantitative Spectroscopy & Radiative
Transfer

5 ABSTRACT

The $\tilde{A}-\tilde{X}$ electronic transition of acetylperoxy radicals ($\text{CH}_3\text{C}(\text{O})\text{O}_2$) in the near-infrared was measured at 67hPa synthetic air in the spectral ranges from 6094 cm^{-1} to 6180 cm^{-1} and 6420 cm^{-1} to 6600 cm^{-1} . $\text{CH}_3\text{C}(\text{O})\text{O}_2$ radicals were generated by the pulsed photolysis of an acetaldehyde/ Cl_2/O_2 mixture at 351 nm and subsequently measured by time-resolved continuous-wave cavity ring-down spectroscopy (cw-CRDS). The absorption cross sections of eight discrete absorption lines were determined relative to the absorption cross section of HO_2 , which has previously been reported. The strongest absorption cross section was found at 6510.73 cm^{-1} and was determined to be $(4.9\pm 2.5) \times 10^{-20}\text{ cm}^2$.

15

INTRODUCTION

In the troposphere, the oxidation of volatile organic compounds (VOCs) is mainly driven by hydroxyl (OH) radicals and leads to the formation of organic peroxy radicals (RO_2). The fate of these RO_2 radicals depends on the chemical composition of the environment. In a polluted atmosphere they react mainly with nitric oxide (NO) to form alkoxy radicals or react with nitrogen dioxide (NO_2) to form peroxy nitrates (RO_2NO_2). Subsequent to the reaction with NO, alkoxy radicals react with O_2 to form hydroperoxy (HO_2) radicals. HO_2 radicals further oxidise NO to NO_2 and regenerate OH closing the quasi-catalytic cycle. The photolysis of produced NO_2 is the only relevant chemical source of tropospheric ozone. In clean environments with low NO_x ($\text{NO}_x = \text{NO} + \text{NO}_2$) concentrations, the dominant loss of RO_2 is due to its reaction with HO_2 forming hydroperoxides ROOH and terminating the radical reaction chain. In addition, RO_2 radicals can react either with other RO_2 as self- ($\text{RO}_2 + \text{RO}_2$) or cross-reaction ($\text{RO}_2 + \text{R}'\text{O}_2$) or with OH radicals ($\text{RO}_2 + \text{OH}$) [1-3].

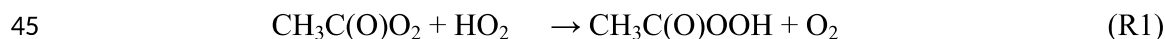
The majority of emitted biogenic non methane hydrocarbons are isoprene (53 %) and monoterpene species (16 %) [4]. The photooxidation of these highly abundant compounds and their oxidation products form among other products also significant amounts of acetylperoxy radicals ($\text{CH}_3\text{C}(\text{O})\text{O}_2$). In the reaction with NO_2 , $\text{CH}_3\text{C}(\text{O})\text{O}_2$ form peroxyacetyl nitrate (PAN) which is a toxic secondary air pollutant. In addition, PAN acts as the principal tropospheric reservoir species for NO_x [5]. The only relevant source in the troposphere is this photochemical

30

35 process, so that PAN is an indicator for photochemical oxidation. Its relatively long atmospheric lifetime of approximately two weeks allows for transport over long distances.

Model calculations of measured radical concentrations in different field studies underestimate HO_x (HO_x = OH + HO₂) radical concentrations in remote regions with high emissions of VOCs from biogenic sources [6-9]. Because acetylperoxy radicals are formed from biogenic precursors and serve as source for HO₂, understanding of its properties is of importance.

Recent studies show that the CH₃C(O)O₂ + HO₂ reaction, which is the most important tropospheric reaction in regions that are dominated by biogenic emissions (low NO emissions), does not only lead to radical chain terminating products (R1, R2), but can also regenerate OH (R3) [10-12]:



This additional OH radical regeneration could improve the model-measurement agreement in low NO_x environments with high VOC emission rates.

50 For an accurate understanding of the CH₃C(O)O₂ + HO₂ reaction, it is necessary to understand the secondary chemistry. For example, the CH₃C(O)O₂ self-reaction (R4) competes with the reaction with HO₂, forming the same product CH₃C(O)O as (R3) making it hard to distinguish between both reactions.



55 In addition, reaction rate constants of the self-reaction ($k_4 = 2.9 \times 10^{-12} \exp(500/T) \text{ cm}^3 \text{ molecule}^{-1} \text{ s}^{-1}$ [13]) and of the reaction with HO₂ ($k_{1-3} = 3.14 \times 10^{-12} \exp(580/T) \text{ cm}^3 \text{ molecule}^{-1} \text{ s}^{-1}$ [13]) are in the same order of magnitude which makes it complicated to study those reaction kinetics.

The detection of RO₂ in previous kinetic laboratory studies was mainly done in the UV region. The spectral overlap of different peroxy species in this region is prone to systematic errors in the quantitative detection [14-18]. Therefore, experiments analysing different RO₂ are difficult to evaluate, if they are detected by UV absorption.

Here, we use absorption of $\text{CH}_3\text{C}(\text{O})\text{O}_2$ in the $\tilde{A}-\tilde{X}$ electronic transition located in the near infrared region. This results in absorption cross sections that are up to several orders of magnitude smaller compared to values in the UV, but the detection is more selective due to less spectral overlap with formed products. In order to measure these small absorption cross sections, very sensitive detection methods need to be used, in our case continuous wave-Cavity Ring Down Spectroscopy (cw-CRDS). While the relative spectrum has already been measured by Zalyubovsky *et al.* [19] in a large wavelength range and the absolute absorption cross section of the strongest band at 5582 cm^{-1} has been estimated, we present here the determination of absolute absorption cross sections in two ranges from $6094\text{ cm}^{-1} - 6180\text{ cm}^{-1}$ and from $6420\text{ cm}^{-1} - 6600\text{ cm}^{-1}$, corresponding to the COO bend and to the OO stretch transition, respectively, relative to the absorption cross section of HO_2 . These cross sections can be used in future works for the quantitative detection of this radical.

EXPERIMENTAL

Experimental setup

The setup has been described in detail before [20-23] and is briefly discussed here (**Figure 1**).

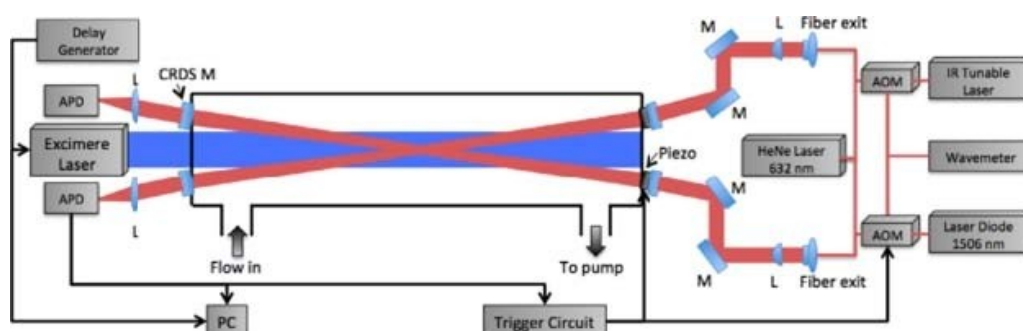


Figure 1. Schematic view of the used experimental setup: AOM, Acousto-Optic Modulator; APD, Avalanche Photo Diode; M, Mirror; L, Lens. Both cw-CRDS systems are equipped with identical trigger circuits and data acquisition systems.

The setup consisted of a 0.79 m long flow reactor made of stainless steel. The beam of a pulsed excimer laser (Lambda Physik LPX 202i) passed the reactor longitudinally. The flow reactor contained two identical continuous wave cavity ring-down spectroscopy (cw-CRDS) absorption paths, which were installed in a small angle with respect to the photolysis path. An overlap with the photolysis beam of 0.377 m is achieved. Both beam paths were tested for a uniform overlap

with the photolysis beam before experiments were done. For this purpose, both cw-CRDS
 90 instruments were operated to simultaneously measure HO₂ concentrations. Deviations between
 HO₂ concentrations were less than 5 % demonstrating that the photolysis laser was very well
 aligned, *i.e.* both light paths probed a very similar photolysed volume in the reactor. A small
 helium purge flow prevented the mirrors from being contaminated. For measuring the
 CH₃C(O)O₂ spectrum, a tunable laser source (Agilent 81680A) was coupled into one of the
 95 cavities by systems of lenses and mirrors. On the other path, a DFB laser was coupled into the
 cavity for the detection of HO₂ radicals during the calibration measurements. The calibration of
 the acetyl peroxy absorption cross section at 6497.94 and 6638.30 cm⁻¹ in 67hPa helium has also
 been carried out using a DFB laser instead of the Agilent module. Each probe beam passed an
 acousto-optic modulator (AOM, AAoptoelectronic) to rapidly turn off the 1st order beam once a
 100 threshold for light intensity in the cavity was reached, in order to measure the ring-down event.
 Then, the decay of light intensity was recorded and an exponential fit is applied to retrieve the
 ring-down time. The absorption coefficient α is derived from Equation (1).

$$\alpha = [A] * \sigma_A = \frac{R_L}{c} \left(\frac{1}{\tau} - \frac{1}{\tau_0} \right) \quad (\text{Eq. 1})$$

where τ is the ring-down time with an absorber present; τ_0 is the ring-down time with no
 105 absorber present; σ_A is the absorption cross section of the absorbing species A; R_L is the ratio
 between cavity length (79 cm) and effective absorption path (37.7 cm); c is the speed of light. To
 calculate the absorption cross section it is necessary to know the absorber concentration.

Acetylperoxy radicals were generated by pulsed 351 nm photolysis of acetaldehyde (CH₃CHO) /
 Cl₂ / O₂ mixtures:



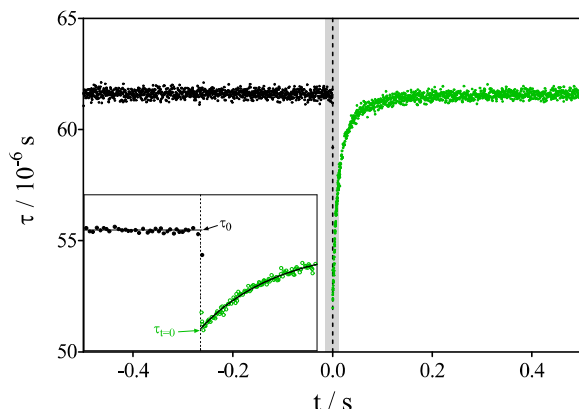
The Cl radical concentration for the measurement of the spectrum was around 1.7×10^{12} cm⁻³ and
 was varied for the calibration measurements between $(1 \text{ and } 8) \times 10^{12}$ cm⁻³. Acetaldehyde was
 115 prepared as a diluted mixture in a glass bulb. A small flow was added to the mixture through a
 calibrated flow meter giving a concentration of 2.5×10^{14} cm⁻³. Nearly all experiments were
 performed in synthetic air, at 298 K and 67hPa total pressure, the absorption cross sections at
 6697.94 and 6638.30 cm⁻¹ were also determined at 67hPa helium. N₂ (Praxair, 4.5), He (Praxair

120 4.5) and O₂ (Praxair, 4.5) were used without further purification. All gas flows were controlled by calibrated mass flow controllers (Bronkhorst, Tylan).

Absorption spectra measurements

125 The procedure to measure absorption spectra has been described before [24, 25] and is only briefly discussed here. The spectrum was measured with a point spacing of 0.1 cm⁻¹ for the wavelength range from 6094 - 6180 cm⁻¹ and 0.2 cm⁻¹ for the wavelength range from 6420 - 6600 cm⁻¹, corresponding to the COO bend and the OO stretch, respectively [19]. Both wavelength regions have been sampled by changing incrementally the wavelength of the laser while a constant amount of CH₃C(O)O₂ was generated in the reactor.

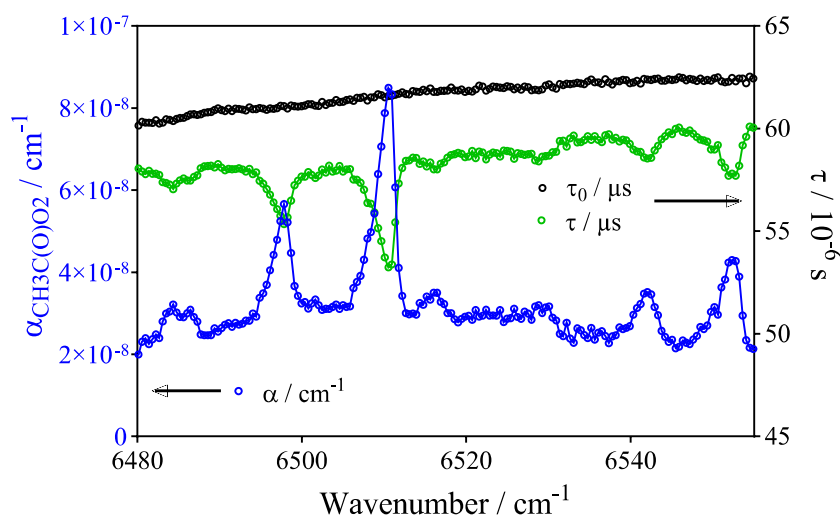
130 For each wavelength, a time series of ring-down measurements testing the acetyperoxy radical absorption was recorded. After the data acquisition was triggered ring-down events were usually recorded 0.5 s each before and after the photolysis laser shot which led to the formation of acetylperoxy radicals. A typical trace is shown in **Figure 2**, where ring-down times from ring-down events occurring before the photolysis pulse are shown in black, and those after the photolysis pulse are shown in green. The loss of CH₃C(O)O₂ radicals is for the first tens of ms
135 mostly due to self-reaction and to the reaction with the radical products of this self-reaction (CH₃O₂ and HO₂). With decreasing radical concentrations on the longer time scale, diffusion out of the photolysis volume becomes the major loss process. To derive the absorbance of the initially produced acetylperoxy radicals, the time-resolved series of ring-down events was extrapolated to the moment of the photolysis pulse (t = 0 s). Different fitting procedures were
140 tested, and it turned out that a bi-exponential fit over the first 50 ms following the photolysis pulse reproduced the data very well and allowed a reliable extrapolation to t = 0 s. However, it has to be kept in mind that the decay of the CH₃C(O)O₂ concentration is due to a complex reaction scheme, and the decay constants from the fit have no physical meaning. The quality of the fit is shown as a black line in the insert of **Figure 2**. τ₀, that is required to calculate the
145 absorbance (Eq. 1), was derived from the average of all detected ring-down events that occurred before the photolysis pulse when no CH₃C(O)O₂ was present. The ring-down events are randomly distributed in time at each photolysis shot because of the random nature of when exactly an efficient coupling of the laser into the cavity was achieved. Ring-down events were therefore accumulated over several laser pulses (10 – 20 generally) to get a better coverage of the
150 whole time range.



155 **Figure 2.** Typical series of ring-down times for $\text{CH}_3\text{C}(\text{O})\text{O}_2$, the insert shows the zoom of the grey-shaded area (± 15 ms). The dashed line represents the time of the photolysis pulse ($t = 0$ s). Ring-down events before the photolysis pulse (black) are used to determine τ_0 , extrapolation to $t=0$ s of a bi-exponential fit of the ring-down times occurring during the first 50 ms after the photolysis pulse (black line in the insert) are used to determine τ .

RESULTS AND DISCUSSION

160 A portion of the relative absorption spectrum of the OO stretch region is shown in **Figure 3**. For each wavenumber, measurements were evaluated as shown in **Figure 2**. Ring-down times extrapolated to $t = 0$ s (green) and τ_0 as the average of all ring-down times before the photolysis pulse (black) are shown for each wavenumber in **Figure 3**. The absorption coefficients (blue) are calculated by applying equation (Eq. 1) to each data pair τ and τ_0 .



165 **Figure 3:** Portion of the relative absorption spectrum: each dot, corresponding to one wavelength, is extracted from a kinetic decay such as shown in **Figure 2**. Black dots represent baseline (τ_0), green dots obtained from extrapolation of bi-exponential fitting such as shown in **Figure 2** ($\tau_{t=0}$), blue dots (α) obtained by applying equation (Eq. 1).

170 In order to convert the absorption coefficient α into absolute cross sections σ , the knowledge of
the exact $\text{CH}_3\text{C}(\text{O})\text{O}_2$ concentration is necessary. Therefore, a series of experiments was
conducted to quantify the initial amount of radicals. This was achieved by quantitatively
converting all Cl-atoms to HO_2 radicals, which can be reliably measured by cw-CRDS on a
strong absorption line at 6638.205 cm^{-1} [23, 26-29]. The measurement of the HO_2 absorption
175 cross section is based on the measurement of HO_2 decays during self-reaction, which allows for
retrieval of the initial concentration, and thus the absorption cross section, if the rate constant is
known. While the uncertainty of the measured HO_2 decays itself is small ($<10\%$), the uncertainty
of the rate constant is currently recommended by the IUPAC committee to $\pm 40\%$. This same
uncertainty has to be considered for the absorption cross sections obtained in this work, as they
180 are measured relative to the HO_2 absorption cross section. The quantitative conversion of Cl-
atoms to HO_2 is done by photolysing a Cl_2 / methanol (CH_3OH) mixture:



Then, CH_3OH is substituted by CH_3CHO to form $\text{CH}_3\text{C}(\text{O})\text{O}_2$ following reactions (R11) and
185 (R12), while keeping conditions for the generation of Cl radicals constant.



Assuming that the concentration of HO_2 radicals corresponds to the concentration of Cl atoms,
the ratio of absorbance measured for $\text{CH}_3\text{C}(\text{O})\text{O}_2$ and HO_2 can be used to calculate the
190 $\text{CH}_3\text{C}(\text{O})\text{O}_2$ absorption cross section relative to the well known HO_2 absorption cross section
according to:

$$\sigma_{\text{CH}_3\text{C}(\text{O})\text{O}_2} = \alpha_{\text{CH}_3\text{C}(\text{O})\text{O}_2} \frac{\sigma_{\text{HO}_2}}{\alpha_{\text{HO}_2}} \quad (\text{Eq. 2})$$

However, the assumption does not entirely apply, because the reaction of $\text{CH}_3\text{CO} + \text{O}_2$ leads also
to the formation of some OH radicals, the yield depending on pressure and nature of the CH_3CO
195 precursor [30-32]. An OH yield of 0.25 is expected in nitrogen at 67hPa [30].



OH radical concentrations can in principle be measured by cw-CRDS in the experimental set-up

[33]. However, concentrations in these experiments were below the limit of detection likely due to the fast reaction with acetaldehyde [13]:



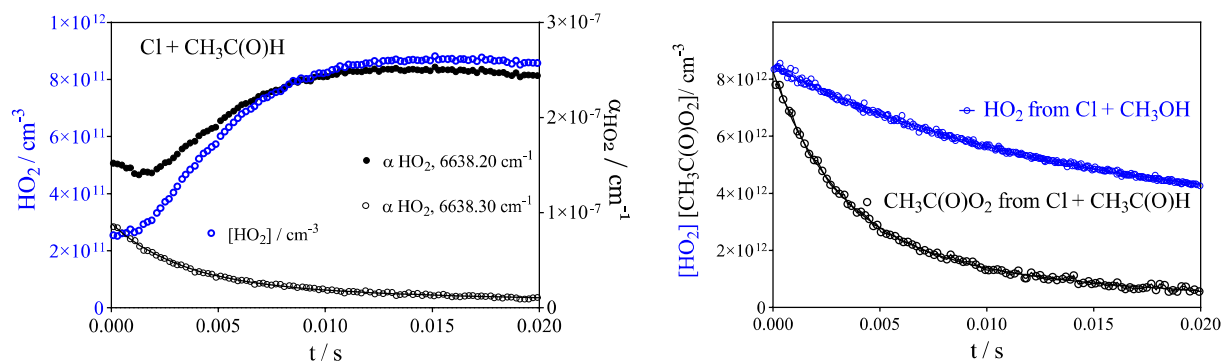
Because under our experimental conditions ($[\text{CH}_3\text{CHO}] = 2.5 \times 10^{14} \text{ cm}^{-3}$), (R13) is leading with $k_{13} = 1.5 \times 10^{-11} \text{ cm}^3 \text{ s}^{-1}$ to an OH lifetime of 250 μs , and can thus, in absence of other potential reaction partners, be considered as the nearly exclusive fate of OH radicals. And because (R13) leads to formation of another CH_3CO radical, this reaction does not introduce an error in the calculation of the absorption cross section using equation (Eq. 2).

205 However, it was observed in our experiments that small amounts of HO_2 radicals are formed immediately from the initial reaction of $\text{CH}_3\text{CHO} + \text{Cl}$. Radical concentrations measured in a typical experiment are shown in **Figure 4**: the left graph shows the HO_2 signal obtained from photolysis of $\text{Cl}_2 / \text{CH}_3\text{CHO} / \text{O}_2$ mixture. Because $\text{CH}_3\text{C}(\text{O})\text{O}_2$ has a broad absorption spectrum [19], it still absorbs in the wavelength range where HO_2 is detected (6638.2 cm^{-1}). Therefore, absolute HO_2 concentrations (blue symbols) are obtained from the difference of the online (6638.2 cm^{-1}) and the offline (6638.3 cm^{-1}) absorption signal. It can be seen that the HO_2 concentration immediately after the photolysis pulse is not zero. The blue symbols on the right graph show the HO_2 concentration time profile under the same conditions, but with CH_3OH instead of CH_3CHO . Comparing the HO_2 concentrations measured from methanol mixtures ($[\text{HO}_2]_{\text{CH}_3\text{OH}}$) and acetaldehyde mixtures ($[\text{HO}_2]_{\text{CH}_3\text{C}(\text{H})\text{O}}$) shows that around 3 % of the Cl-atoms are converted to HO_2 (δ_{HO_2}) in the presence of CH_3CHO .

$$215 \quad \delta_{\text{HO}_2} = \frac{[\text{HO}_2]_{\text{CH}_3\text{CHO}}}{[\text{HO}_2]_{\text{CH}_3\text{OH}}} \quad (3)$$

This small correction of the initial $\text{CH}_3\text{C}(\text{O})\text{O}_2$ concentration was taken into account when converting the absorption coefficient of $\text{CH}_3\text{C}(\text{O})\text{O}_2$ into absorption cross sections:

$$220 \quad \sigma_{\text{CH}_3\text{C}(\text{O})\text{O}_2} = \alpha_{\text{CH}_3\text{C}(\text{O})\text{O}_2} \frac{\sigma_{\text{HO}_2}}{\alpha_{\text{HO}_2}} \times \frac{1}{(1 - \delta_{\text{HO}_2})} \quad (4)$$



225 **Figure 4:** Left plot shows HO₂ absorption coefficient online (6638.20 cm⁻¹, black dots) and offline (6638.30 cm⁻¹, open black symbols, right y-axis apply for both) and HO₂ concentration (blue symbols, left y-axis) measured after photolysing a Cl₂/ CH₃CHO / O₂ mixture. Right graph shows the HO₂ concentration from the photolysis of Cl₂/ CH₃OH / O₂ mixture (blue symbols) and the CH₃C(O)O₂ concentration time profile from the photolysis of the Cl₂/ CH₃CHO/ O₂ mixture (black symbols). Both experiments used the same Cl₂ concentration.

230 The origin of this rapid HO₂ formation is not clear, but is formed possibly through the reaction



Such a rapid HO₂ formation with similar yields had already been observed by Morajkar et al.[34] with a yield of around 7%, independent of pressure between 10 and 90 Torr helium, following the 248 nm photolysis of CH₃CHO, and also by Hui et al.[35] with a yield of 2-3% following the reaction of Cl-atoms with CH₃CHO at 100 Torr N₂. HO₂ concentrations at 67 hPa N₂ have been calculated using an absorption cross section of $\sigma_{\text{HO}_2, 6638.20\text{cm}^{-1}} = 2.01 \times 10^{-19} \text{ cm}^2$, obtained from the empirical expression of Assaf *et al.*[27].

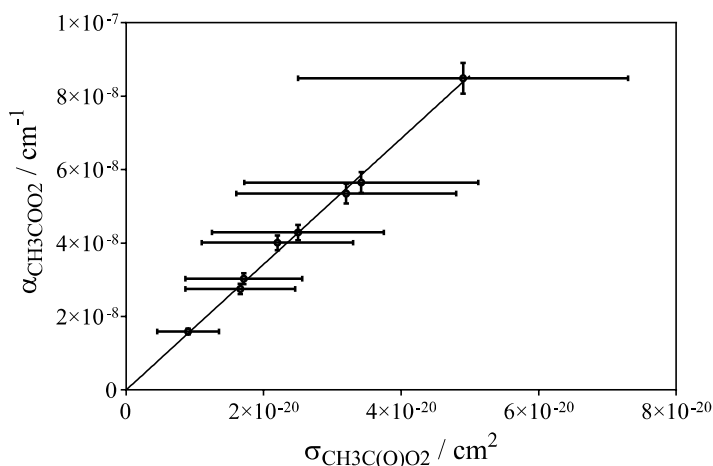
240 This way, absorption cross sections σ were measured for 8 wavenumbers in synthetic air and for 2 wavenumbers in helium, given in **Table 1** together with the absorption coefficients α for the same wavelengths in synthetic air, such as found during the measurement of the full spectrum. Also given in **Table 1** are the absorption cross sections for two wavenumbers, obtained in 67 hPa helium: 6697.94 cm⁻¹ corresponds to one peak of the OO-stretch transition band, while 6638.30 cm⁻¹ corresponds to the wavenumber that we commonly use for the measurement of the HO₂-offline signal, i.e. the open circles in **Figure 4**. The error bars of the absorption coefficients α are statistical only and are given with $\pm 5\%$, obtained from the 95% confidence interval of the extrapolation of the bi-exponential fit to $t = 0\text{s}$ (black curve in the insert of **Figure 2**, typically below 4%) as well as the τ_0 (average of all ring down events before the photolysis pulse: typically less than 1%). The error bars for the absorption cross sections are given with $\pm 50\%$ and are composed of twice the uncertainty of extrapolating α to $t = 0\text{s}$ (once for $\alpha_{\text{CH}_3\text{C(O)O}_2}$ and once for

250 α_{HO_2}) and the 40% uncertainty given by the IUPAC committee[36] for the rate constant of the
 HO₂ self-reaction, that was used to determine the absorption cross section of HO₂.

255 **Table 1:** Absorption coefficient α for CH₃C(O)O₂ from the measurement of the full spectrum for eight
 wavenumbers (marked by lines in the full spectrum of **Figure 6**) and absorption cross sections σ for the
 same lines, determined relative to the HO₂ cross section at 67 hPa N₂ and for two wavenumbers at 67 hPa
 helium

Wavenumber / cm ⁻¹	$\alpha / 10^{-8} \text{ cm}^{-1}$	$\sigma / 10^{-20} \text{ cm}^2$
6121.08	5.65±0.28	3.4±1.7
6164.75	2.75±0.14	1.7±0.8
6108.74	4.01±0.20	2.2±1.1
6114.53	1.59±0.08	0.9±0.5
6497.94	5.35±0.27	3.2±1.6
6697.94 (helium)		3.3±1.7
6502.80	3.03±0.15	1.7±0.9
6552.76	4.29±0.21	2.5±1.3
6510.74	8.49±0.42	4.9±2.4
6638.30 (helium)		0.8±0.4

In **Figure 5** the absorption coefficients are plotted for all eight wavenumbers as a function of the
 absorption cross sections σ . A good linearity is found, assuring that the CH₃C(O)O₂
 260 concentration was stable during the measurement of the full spectrum.



265 **Figure 5:** Absorption coefficients α as a function of the absorption cross sections σ from **Table 1**. Error
 bars are statistical for absorption coefficients α (5%), and an uncertainty of 45% is added for the
 absorption cross section σ , taking into account the uncertainty in the absorption cross section for HO₂.

The slope from the linear regression of **Figure 5** leads to the concentration of $\text{CH}_3\text{C}(\text{O})\text{O}_2$ radicals that was generated during the measurement of the full spectrum: $1.7 \times 10^{12} \text{ cm}^{-3}$. This value was used for the conversion of the absorption coefficients from the relative spectra (blue line in **Figure 3**) of the two wavelength ranges into absolute absorption cross sections, shown in **Figure 6**. A comparison with a previously published spectrum [19] shows an excellent agreement of the positions and relative intensities of the different absorption maxima.

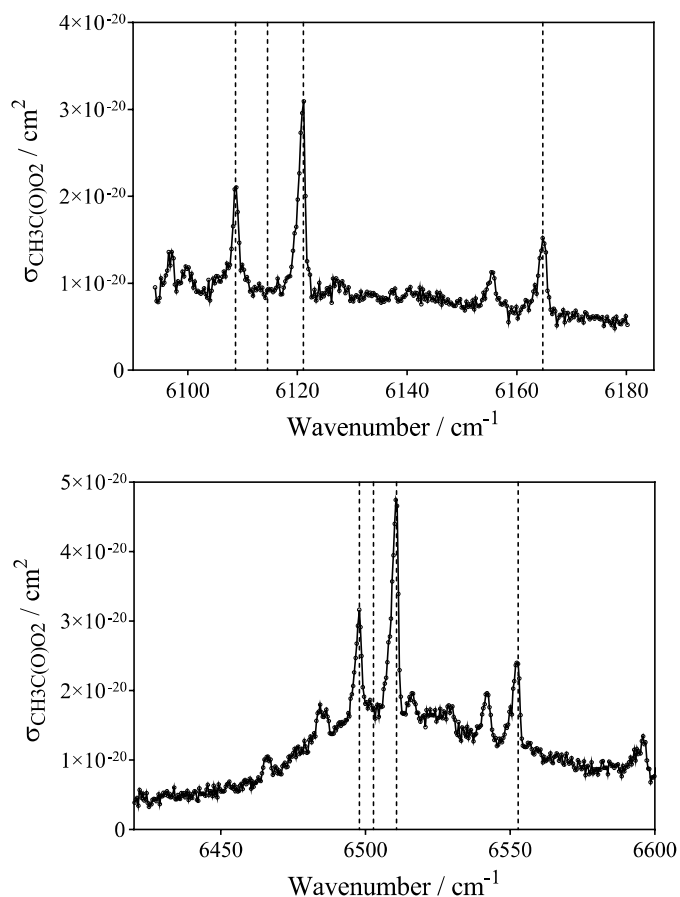


Figure 6: Absolute absorption spectrum of $\text{CH}_3\text{C}(\text{O})\text{O}_2$. Vertical lines indicate the wavelengths where absolute absorption cross sections have been determined relative to the absorption cross section of HO_2 (see **Table 1**). The data can be downloaded as supplementary data.

Zalyubovsky *et al.* [19] determined an absorption cross section of $\sigma = (1 \pm 0.5) \times 10^{-19} \text{ cm}^2$ at 5582.5 cm^{-1} . This is consistent with our absorption cross section of $(4.9 \pm 2.4) \times 10^{-20} \text{ cm}^2$ at the absorption maximum 6510.71 cm^{-1} , which has in the spectrum of Zalyubovsky *et al.* a relative intensity of approximately a factor 2 less than the absorption maximum at 5582.5 cm^{-1} .

The results obtained in this work will be used in future studies on the reaction kinetics of $\text{CH}_3\text{C}(\text{O})\text{O}_2$ radicals. Depending on the quality of alignment, cleanliness of mirrors, etc. a decrease of the ring-down time of $\Delta\tau = 0.5 \mu\text{s}$ on a typical $\tau_0 = 50 \mu\text{s}$ can be achieved in time-resolved experiments, leading to a limit of detection below $[\text{CH}_3\text{C}(\text{O})\text{O}_2] = 4 \times 10^{11} \text{ cm}^{-3}$, making this technique more sensitive than typical UV-absorption measurements. And even though the spectrum features a rather broad background, *i.e.* lacks the high selectivity that can be achieved for HO_2 or OH measurements, its main absorption peaks are red-shifted compared to other small peroxy radicals such as HO_2 , CH_3O_2 [24, 37, 38], $\text{C}_2\text{H}_5\text{O}_2$ [37] and should thus allow a selective detection for measuring the rate constants and branching ratios of self- and cross-reactions.

295 CONCLUSION

We measured the $\text{CH}_3\text{C}(\text{O})\text{O}_2$ absorption spectrum in the ranges from 6094 cm^{-1} - 6180 cm^{-1} and 6420 cm^{-1} - 6600 cm^{-1} . Measurements were performed in 67hPa synthetic air or helium total pressure. Radicals were generated by the pulsed photolysis of acetaldehyde / Cl_2 / O_2 mixtures at 351 nm.

300 Some large peaks on top of a broad absorption spectrum were obtained, in good agreement with an earlier measurement by Zalyubovsky *et al.* [19]. Absolute absorption cross sections were measured for eight different wavelengths and are in good agreement relative to the only available measurement by Zalyubovsky *et al.* [19] performed at a lower wavenumber.

305 Acknowledgements

This project was supported by the French ANR agency under contract No. ANR-11-Labx-0005-01 CaPPA (Chemical and Physical Properties of the Atmosphere), the Région Hauts-de-France, the Ministère de l'Enseignement Supérieur et de la Recherche (CPER Climibio) and the European Fund for Regional Economic Development. This project has received funding from the European Research Council (ERC) under the European Union's Horizon 2020 research and innovation programme (SARLEP grant agreement No. 681529) and from the exchange program of the Deutscher Akademischer Austauschdienst (DAAD) (project number 57316518) and PHC Procope project no. 37666WA.

REFERENCES

- [1] Orlando JJ, Tyndall GS. Laboratory studies of organic peroxy radical chemistry: an overview with emphasis on recent issues of atmospheric significance. *Chem Soc Rev.* 2012;41:6294-317.
- 320 [2] Fittschen C. The reaction of peroxy radicals with OH radicals. *Chem Phys Lett.* 2019;725:102-8.
- [3] Assaf E, Song B, Tomas A, Schoemaeker C, Fittschen C. Rate Constant of the Reaction between CH_3O_2 Radicals and OH Radicals revisited. *J Phys Chem A.* 2016;120:8923-32.
- [4] Guenther AB, Jiang X, Heald CL, Sakulyanontvittaya T, Duhl T, Emmons LK, et al. The Model
325 of Emissions of Gases and Aerosols from Nature version 2.1 (MEGAN2. 1): an extended and updated framework for modeling biogenic emissions. *Geosci Model Dev.* 2012;5:1471-92.
- [5] Fischer EV, Jacob DJ, Yantosca RM, Sulprizio MP, Millet DB, Mao J, et al. Atmospheric peroxyacetyl nitrate (PAN): a global budget and source attribution. *Atmos Chem Phys.* 2014;14:2679-98.
- 330 [6] Tan D, Faloon I, Simpas JB, Brune W, Shepson PB, Couch TL, et al. HO_x budgets in a deciduous forest: Results from the PROPHET summer 1998 campaign. *J Geophys Res Atmos.* 2001;106:24407-27.
- [7] Lelieveld J, Butler TM, Crowley JN, Dillon TJ, Fischer H, Ganzeveld L, et al. Atmospheric oxidation capacity sustained by a tropical forest. *Nature.* 2008;452:737-40.
- 335 [8] Hofzumahaus A, Rohrer F, Lu K, Bohn B, Brauers T, Chang CC, et al. Amplified trace gas removal in the troposphere. *Science.* 2009;324:1702-4.
- [9] Wolfe GM, Thornton JA, Bouvier-Brown NC, Goldstein AH, Park JH, McKay M, et al. The Chemistry of Atmosphere-Forest Exchange (CAFE) Model - Part 2: Application to BEARPEX-2007 observations. *Atmos Chem Phys.* 2011;11:1269-94.
- 340 [10] Hasson AS, Tyndall GS, Orlando JJ. A Product Yield Study of the Reaction of HO_2 Radicals with Ethyl Peroxy ($\text{C}_2\text{H}_5\text{O}_2$), Acetyl Peroxy ($\text{CH}_3\text{C}(\text{O})\text{O}_2$), and Acetonyl Peroxy ($\text{CH}_3\text{C}(\text{O})\text{CH}_2\text{O}_2$) Radicals. *J Phys Chem A.* 2004;108:5979-89.
- [11] Winiberg FAF, Dillon TJ, Orr SC, Groß CBM, Bejan I, Brumby CA, et al. Direct measurements of OH and other product yields from the $\text{HO}_2 + \text{CH}_3\text{C}(\text{O})\text{O}_2$ reaction. *Atmos Chem Phys.* 2016;16:4023-42.
- 345 [12] Hui AO, Fradet M, Okumura M, Sander SP. Temperature Dependence Study of the Kinetics and Product Yields of the $\text{HO}_2 + \text{CH}_3\text{C}(\text{O})\text{O}_2$ Reaction by Direct Detection of OH and HO_2 Radicals Using 2f-IR Wavelength Modulation Spectroscopy. *J Phys Chem A.* 2019;123:3655-71.
- [13] Atkinson R, Baulch DL, Cox RA, Crowley JN, Hampson RF, Hynes RG, et al. Evaluated kinetic and photochemical data for atmospheric chemistry: Volume II - gas phase reactions of organic
350 species. *Atmos Chem Phys.* 2006;6:3625-4055.
- [14] Addison MC, Burrows JP, Cox RA, Patrick R. ABSORPTION-SPECTRUM AND KINETICS OF THE ACETYLPEROXY RADICAL. *Chem Phys Lett.* 1980;73:283-7.
- [15] Moortgat G, Veyret B, Lesclaux R. ABSORPTION-SPECTRUM AND KINETICS OF REACTIONS
355 OF THE ACETYLPEROXY RADICAL. *J Phys Chem.* 1989;93:2362-8.
- [16] Lightfoot PD, Cox RA, Crowley JN, Destriau M, Hayman GD, Jenkin ME, et al. ORGANIC PEROXY-RADICALS - KINETICS, SPECTROSCOPY AND TROPOSPHERIC CHEMISTRY. *Atmospheric Environment Part a-General Topics.* 1992;26:1805-961.
- 360 [17] Roehl CM, Bauer D, Moortgat GK. Absorption spectrum and kinetics of the acetylperoxy radical. *J Phys Chem.* 1996;100:4038-47.

- [18] Maricq MM, Sente JJ. The $\text{CH}_3\text{C}(\text{O})\text{O}_2$ Radical. Its UV Spectrum, Self-Reaction Kinetics, and Reaction with CH_3O_2 . *J Phys Chem*. 1996;100:4507-13.
- [19] Zalyubovsky SJ, Glover BG, Miller TA. Cavity Ringdown Spectroscopy of the $\tilde{A} - \tilde{X}$ Electronic Transition of the $\text{CH}_3\text{C}(\text{O})\text{O}_2$ Radical. *J Phys Chem A*. 2003;107:7704-12.
- 365 [20] Thiebaud J, Fittschen C. Near Infrared cw-CRDS Coupled to Laser Photolysis: Spectroscopy and Kinetics of the HO_2 Radical. *Appl Phys B*. 2006;85:383-9.
- [21] Parker AE, Jain C, Schoemaeker C, Szriftgiser P, Votava O, Fittschen C. Simultaneous, time-resolved measurements of OH and HO_2 radicals by coupling of high repetition rate LIF and cw-CRDS techniques to a laser photolysis reactor and its application to the photolysis of H_2O_2 .
- 370 *Appl Phys B*. 2011;103:725-33.
- [22] Votava O, Mašát M, Parker AE, Jain C, Fittschen C. Microcontroller based resonance tracking unit for time resolved continuous wave cavity-ringdown spectroscopy measurements. *Rev Sci Instrum*. 2012;83:043110.
- [23] Assaf E, Asvany O, Votava O, Batut S, Schoemaeker C, Fittschen C. Measurement of line strengths in the $\tilde{A} 2A' \leftarrow X 2A''$ transition of HO_2 and DO_2 . *J Quant Spectrosc Radiat Transfer*. 2017;201:161-70.
- 375 [24] Faragó EP, Viskolcz B, Schoemaeker C, Fittschen C. Absorption Spectrum and Absolute Absorption Cross Sections of CH_3O_2 Radicals and CH_3I Molecules in the Wavelength Range 7473–7497 cm^{-1} . *J Phys Chem A*. 2013;117:12802-11.
- 380 [25] Jain C, Morajkar P, Schoemaeker C, Viskolcz B, Fittschen C. Measurement of Absolute Absorption Cross Sections for Nitrous Acid (HONO) in the Near-Infrared Region by the continuous wave Cavity Ring-Down Spectroscopy (cw-CRDS) Technique coupled to Laser Photolysis. *J Phys Chem A*. 2011;115:10720-8.
- [26] Thiebaud J, Crunaire S, Fittschen C. Measurements of Line Strengths in the $2\nu_1$ Band of the HO_2 Radical Using Laser Photolysis/Continuous Wave Cavity Ring-Down Spectroscopy (cw-CRDS). *J Phys Chem A*. 2007;111:6959-66.
- 385 [27] Assaf E, Liu L, Schoemaeker C, Fittschen C. Absorption spectrum and absorption cross sections of the $2\nu_1$ band of HO_2 between 20 and 760 Torr air in the range 6636 and 6639 cm^{-1} . *Journal of Quantitative Spectroscopy & Radiative Transfer*. 2018;211:107-14.
- 390 [28] Onel L, Brennan A, Gianella M, Ronnie G, Lawry Aguila A, Hancock G, et al. An intercomparison of HO_2 measurements by fluorescence assay by gas expansion and cavity ring-down spectroscopy within HIRAC (Highly Instrumented Reactor for Atmospheric Chemistry). *Atmos Meas Tech*. 2017;10:4877-94.
- [29] Tang Y, Tyndall GS, Orlando JJ. Spectroscopic and Kinetic Properties of HO_2 Radicals and the Enhancement of the HO_2 Self Reaction by CH_3OH and H_2O . *J Phys Chem A*. 2010;114:369-78.
- 395 [30] Groß CBM, Dillon TJ, Crowley JN. Pressure dependent OH yields in the reactions of CH_3CO and HOCH_2CO with O_2 . *Phys Chem Chem Phys*. 2014;16:10990-8.
- [31] Carr SA, Baeza-Romero MT, Blitz MA, Pilling MJ, Heard DE, Seakins PW. OH yields from the $\text{CH}_3\text{CO} + \text{O}_2$ reaction using an internal standard. *Chem Phys Lett*. 2007;445:108-12.
- 400 [32] Devolder P, Dusanter S, Lemoine B, Fittschen C. About the Co-Product of the OH Radical in the Reaction of Acetyl with O_2 below Atmospheric Pressure. *Chem Phys Lett*. 2006;417:154-8.
- [33] Assaf E, Fittschen C. Cross Section of OH Radical Overtone Transition near 7028 cm^{-1} and Measurement of the Rate Constant of the Reaction of OH with HO_2 Radicals. *J Phys Chem A*. 2016;120:7051-9.
- 405

- [34] Morajkar P, Bossolasco A, Schoemaeker C, Fittschen C. Photolysis of CH₃CHO at 248 nm: Evidence of Triple Fragmentation from Primary Quantum Yield of CH₃ and HCO Radicals and H Atoms. *J Chem Phys.* 2014;140:214308.
- 410 [35] Hui AO, Fradet M, Okumura M, Sander SP. Temperature Dependence Study of the Kinetics and Product Yields of the HO₂ + CH₃C(O)O₂ Reaction by Direct Detection of OH and HO₂ Radicals Using 2f-IR Wavelength Modulation Spectroscopy. *J Phys Chem A.* 2019;123:3655-71.
- 415 [36] Atkinson R, Baulch DL, Cox RA, Crowley JN, Hampson RF, Hynes RG, et al. Evaluated Kinetic and Photochemical Data for Atmospheric Chemistry: Volume 1 – Gas Phase Reactions of O_x, HO_x, NO_x, and SO_x, Species, IUPAC Task Group on Atmospheric Chemical Kinetic Data Evaluation, <http://iupac.pole-ether.fr>. " Vol 2. *Atmos Chem Phys.* 2004;4:1461-738.
- [37] Atkinson DB, Hudgens JW. Chemical Kinetic Studies Using Ultraviolet Cavity Ring-Down Spectroscopic Detection: Self-Reaction of Ethyl and Ethylperoxy Radicals and the Reaction O₂ + C₂H₅ → C₂H₅O₂. *J Phys Chem A.* 1997;101:3901-9.
- 420 [38] Chung C-Y, Cheng C-W, Lee Y-P, Liao H-Y, Sharp EN, Rupper P, et al. Rovibronic bands of the $\tilde{A} \leftarrow \tilde{X}$ transition of CH₃OO and CD₃OO detected with cavity ringdown absorption near 1.2–1.4 μm. *J Chem Phys.* 2007;127:044311.